

Deterministic Space-Frequency Nulling for Large Wideband Arrays (DRAFT)

Steven W. Ellingson¹

¹ The Ohio State University ElectroScience Laboratory, 1320 Kinnear Road, Columbus OH 43212. E-mail: ellingson.1@osu.edu

Abstract

Abstract.

I. INTRODUCTION

Intro.

II. THEORY

Consider an array of N antenna elements, which is being used to point at beam in the direction $\hat{\mathbf{r}}(t)$. To accomplish this following procedure is followed (see [1] for a detailed discussion):

1. The signal from each element is downconverted from the original center frequency ω_c of the observation to a center frequency of zero; i.e., to “lowpass” or “complex baseband” form.
2. If the array is large and $\hat{\mathbf{r}}(t)$ varies with time, then it is necessary to perform “fringe stopping”; i.e., applying a time-varying phase $\theta_n(t) = \omega_c \tau_n(t)$ where $\tau_n(t)$ is the geometrical delay associated with a plane wave incident from the direction in which $\hat{\mathbf{r}}(t)$ points. This ensures that the array outputs add coherently. Since phase shifts are preserved in downconversions, fringe stopping may be applied before, during, or after downconversion.
3. Each array output is individually delayed to equalize the geometrical delays $\tau_n(t)$ associated with $\hat{\mathbf{r}}(t)$ for each element n .
4. It may be necessary to equalize the spectrum of the element outputs before summing, in order to account for differences in the frequency responses of the antennas. If the frequency response of the n^{th} antenna in direction $\hat{\mathbf{r}}$ (now dropping the explicit display of time dependence) is $G_n(\omega + \omega_c; \hat{\mathbf{r}})$, this entails convolution by $\mathcal{F}^{-1} \{G_n^{-1}(\omega + \omega_c; \hat{\mathbf{r}})\}$. In practice, it is often a good approximation to assume $G_n(\omega + \omega_c; \hat{\mathbf{r}})$ is simply a complex coefficient (i.e., frequency invariant).
5. It may also be necessary to equalize the spectrum of the element outputs before summing, in order to account for differences in the frequency responses of the signal path following the antennas themselves. If the frequency response of the receiver for the n^{th} element is $C_n(\omega)$, this entails convolution by $\mathcal{F}^{-1} \{C_n^{-1}(\omega)\}$. In practice, it is often a good approximation to assume $C_n(\omega)$ is simply a complex coefficient (i.e., frequency invariant).

6. Finally, the processed signals from each element are summed.

It is shown in [1] that the output of the n^{th} element after Step 3 above is given by

$$V_n(\omega; \hat{\mathbf{r}}) = C_n(\omega)G_n(\omega + \omega_c; \hat{\mathbf{r}})S(\omega) \quad (1)$$

where $S(\omega)$ is the baseband (possibly complex-valued) version of the spectrum of the source signal incident from the direction in which $\hat{\mathbf{r}}$ points. Now the beamforming operation can be described as follows:

$$Y(\omega; \hat{\mathbf{r}}) = \sum_{n=1}^N W_n(\omega)V_n(\omega; \hat{\mathbf{r}}) \quad (2)$$

To obtain the beam that maximizes gain in the direction $\hat{\mathbf{r}}(t)$ subject to no other constraints, one chooses

$$W_n(\omega) = C_n^{-1}(\omega)G_n^{-1}(\omega + \omega_c; \hat{\mathbf{r}}) \quad (3)$$

but if the C_n 's and G_n 's are approximately frequency invariant (as mentioned above), it is more convenient to use (for example),

$$W_n = C_n^{-1}(0)G_n^{-1}(\omega_c; \hat{\mathbf{r}}) \quad (4)$$

which reduces the beamforming operation to multiplication by coefficients followed by summing. For the remainder of this paper, we will restrict our attention to beamforming architectures in which the W_n are coefficients.

Note that Equation 1 applies only to a point source in the direction in which the beam points. For a point source in the m^{th} arbitrary direction $\hat{\mathbf{k}}_m$, the result is

$$V_n(\omega; \hat{\mathbf{k}}_m) = C_n(\omega)G_n(\omega + \omega_c; \hat{\mathbf{k}}_m)S(\omega)e^{j(\omega+\omega_c)(\tau_n-\tau_n^{(m)})} \quad (5)$$

where $\tau_n^{(m)}$ is the geometrical delay associated with the direction $\hat{\mathbf{k}}_m$ for the n element, and τ_n continues to refer to the geometrical delay associated with the beam pointing direction $\hat{\mathbf{r}}$. Equation 5 confirms that even perfectly-implemented delay-and-sum beamforming results in spectral distortion (“bandwidth smearing”) for signals incident from any direction other than the main beam pointing direction *even within the main lobe of the array pattern*.

We now state the problem we wish to solve in this paper. In lieu of the beamforming coefficients W_n from Equation 4, we wish to find an alternative set of coefficients U_n which

yield the same beam pattern values as the W_n 's at M_1 space-frequency points $(\omega_m, \hat{\mathbf{k}}_m)$:

$$\sum_{n=1}^N U_n V_n(\omega_m; \hat{\mathbf{k}}_m) = Y(\omega_m; \hat{\mathbf{r}}) , \quad m = 1 \dots M_1 \quad (6)$$

while simultaneously yielding different, specified beam pattern values at M_2 other space-frequency points:

$$\sum_{n=1}^N U_n V_n(\omega_m; \hat{\mathbf{k}}_m) = A_m , \quad m = M_1 + 1 \dots M \quad (7)$$

where $M = M_1 + M_2$ is the total number of constrained space-frequency points. Note, for example, that a null can be specified as $A_m = 0$. Another example is that bandwidth smearing and variations in the system frequency response can be exactly corrected at a single space-frequency point using

$$A_m = C_n^{-1}(\omega_m) G_n^{-1}(\omega_m + \omega_c; \hat{\mathbf{k}}_m) e^{-j(\omega_m + \omega_c)(\tau_n - \tau_n^{(m)})} \quad (8)$$

A third example is that A_m might be set to a fixed value over an extended period of time to fix the array response over that period. This may be useful in self-calibration; i.e., the array response for calibration point sources could be held fixed for an arbitrarily-long time period.

Equations 6 and 7 yield a system of linear equations in the form

$$\mathbf{V}\mathbf{u} = \mathbf{a} \quad (9)$$

where \mathbf{V} is the $M \times N$ matrix whose (n^{th}, m^{th}) element is

$$[\mathbf{V}]_{mn} = C_n^{-1}(\omega_m) G_n^{-1}(\omega_m + \omega_c; \hat{\mathbf{k}}_m) , \quad (10)$$

$$\mathbf{u} = [U_1 \dots U_N]^T , \quad \text{and} \quad (11)$$

$$\mathbf{a} = [Y(\omega_1; \hat{\mathbf{r}}) \dots Y(\omega_{M_1}; \hat{\mathbf{r}}) A_{M_1+1} \dots A_M]^T , \quad (12)$$

where the superscript “ T ” denotes the transpose.

The proposed solution to Equation 9 is

$$\mathbf{u} = \mathbf{V}^H (\mathbf{V}\mathbf{V}^H)^{-1} \mathbf{a} , \quad (13)$$

where the superscript “ H ” denotes the conjugate transpose. Thus, it is possible to obtain deterministically a beamformer which conforms to the original “prototype” beamformer

(given by the coefficients W_n) at M_1 space-frequency points and conforms to the user's specified values (A_m) at M_2 other space-frequency points. Furthermore, it should be noted that this beamformer is very easy to compute: for $M \ll N$, the computational burden is not dominated by the matrix inversion (which requires $\mathcal{O}(M^3)$ multiplies), but rather by the multiplication of $M \times N$ rectangular matrices.

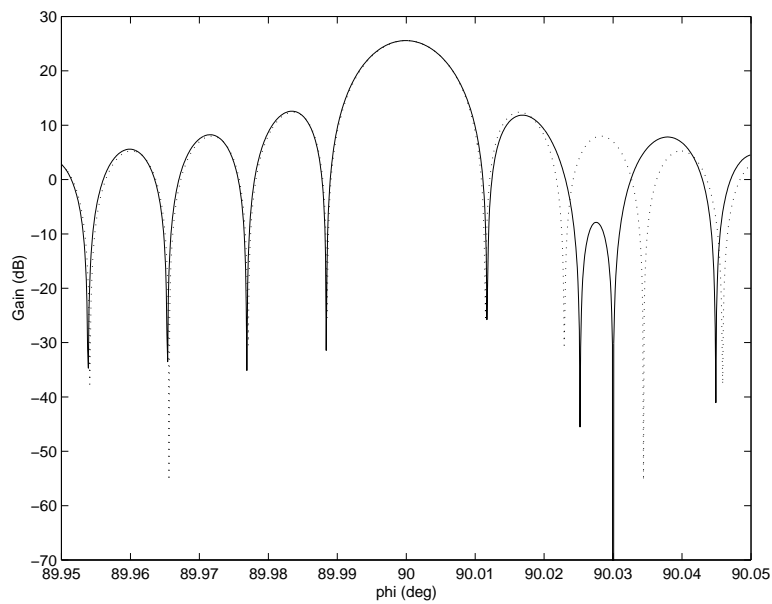
III. EXAMPLE

Consider the following example: An array consists of $N = 19$ elements with isotropic patterns, spaced 55 m apart along a straight line, such that the maximum baseline of the array is about 1 km long. The “prototype” beamforming coefficients $W_n = 1$ result in a beam that has the maximum possible gain in zenith direction 90° subject to no other constraints. The resulting pattern at 1420 MHz is shown in Figure 1(a) and the frequency response in the beam pointing direction is shown in Figure 2(a).

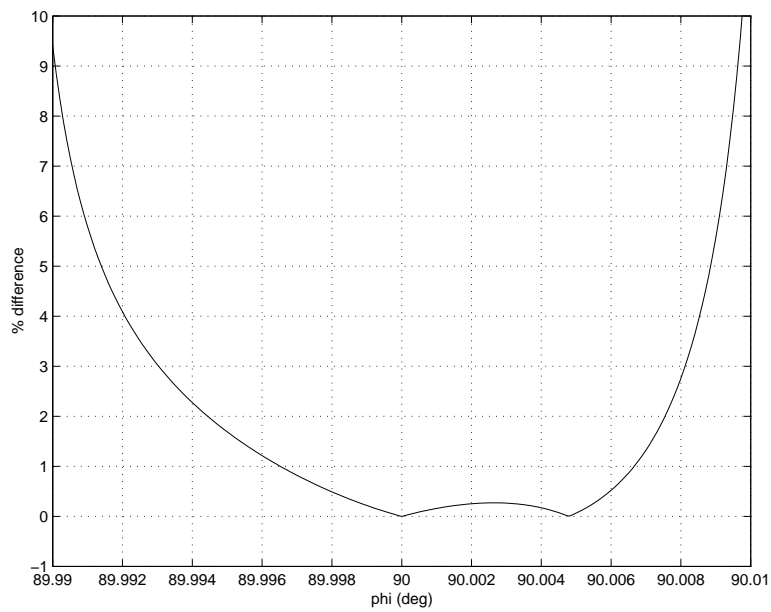
Next, we use the proposed procedure with $M = 2$ to form a new beam. The $m = 1$ constraint is fixed the beam in the original look direction with a gain equal to N , and the $m = 2$ is to drive a perfect null at $(90.03^\circ, 1420 \text{ MHz})$. The resulting pattern is shown in Figure 1(a). Note that the two constraints are met, and furthermore the perturbation of the pattern is slight, especially for the main lobe. Figure 1(b) shows the pattern magnitude error for the main lobe; note that the error is less than 1% over much of the main lobe, especially close to the pointing direction. Figures 2(a) and (b) show the frequency response for the new beamformer in the pointing direction and null direction, respectively. Note that there is no distortion in the pointing direction, and that the null is relatively narrow in frequency; just a few MHz.

Next, we use the proposed procedure to add two more nulls (now, $M = 4$), both also at 1420 MHz, but located at 90.035° and 90.04° respectively. Figures 3 show that the nulls are properly placed and that the main lobe distortion remains small. The frequency response is not shown, but is quite similar to that shown in Figure 2(a) and (b) for a single null; i.e., negligible main lobe distortion, very narrowband nulls.

Finally, consider the case where $M = 4$, but the three nulls are at the same location – 90.03° – but at three different frequencies: 1410 MHz, 1420 MHz, and 1430 MHz. The results are shown in Figures 4 and 5. Once again, we see the nulls are properly placed.

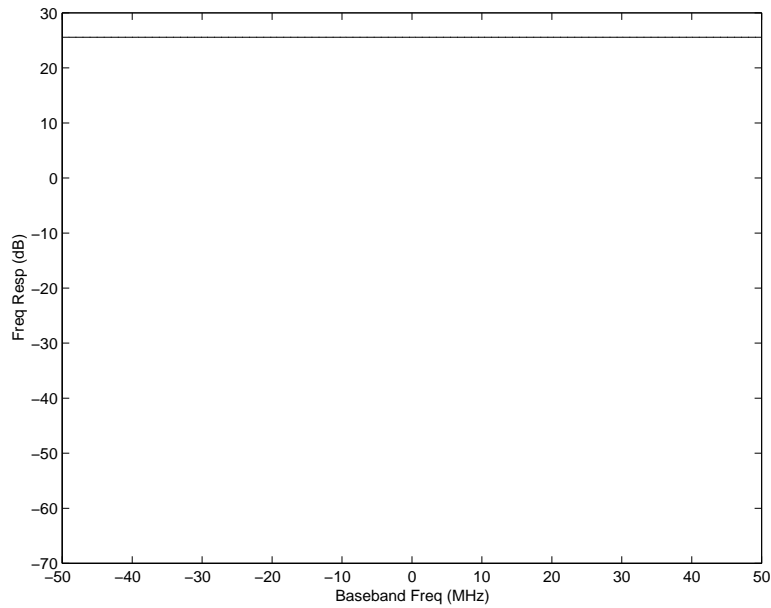


(a) Pattern. *Solid: New, Dash: Prototype.*

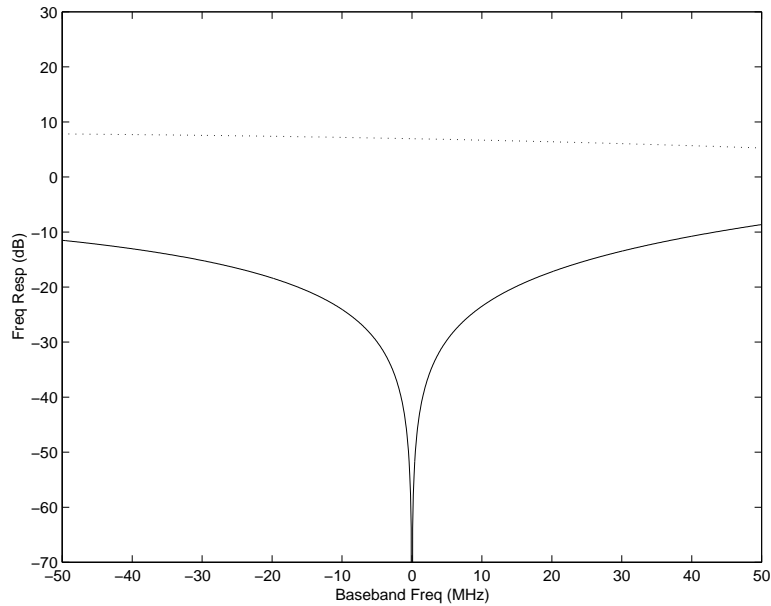


(b) Pattern error in main lobe.

Fig. 1. One null at $(90.03^\circ, 1420 \text{ MHz})$; 1420 MHz pattern results.

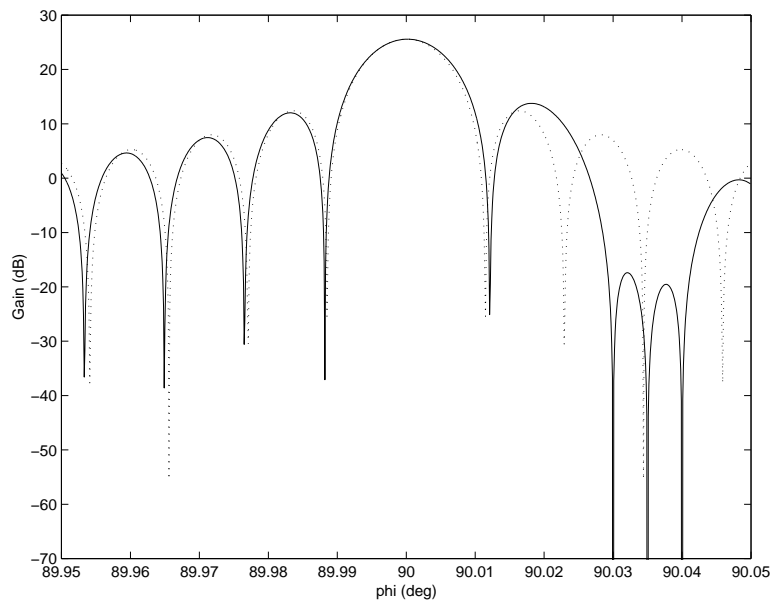


(a) Frequency Response at 90.0° . *Solid*: New, *Dash*: Prototype.

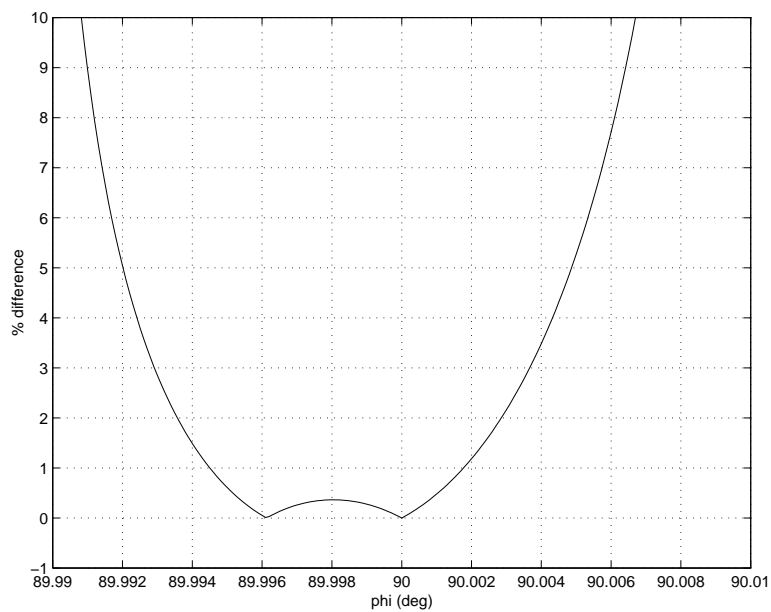


(b) Frequency Response at 90.03° . *Solid*: New, *Dash*: Prototype.

Fig. 2. One null at $(90.03^\circ, 1420 \text{ MHz})$; Frequency Response.



(a) Pattern. *Solid: New, Dash: Prototype.*



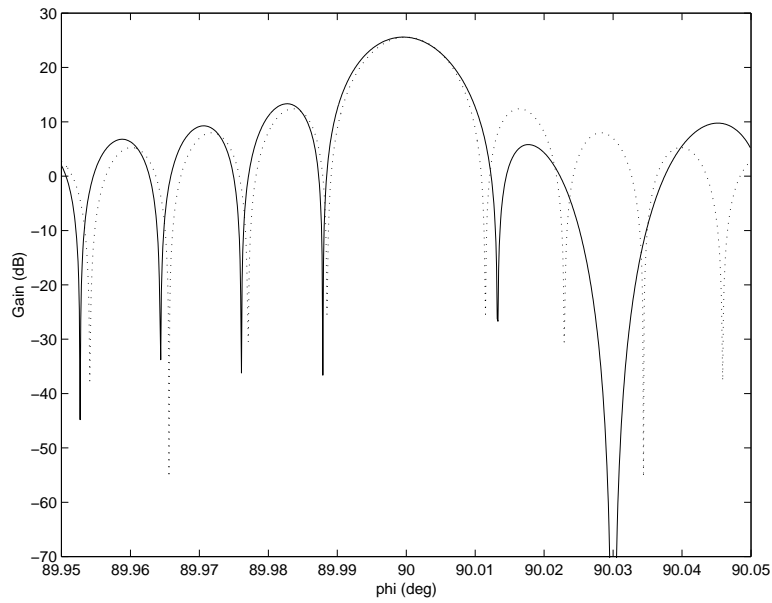
(b) Pattern error in main lobe.

Fig. 3. Three nulls: $(90.03^\circ, 1420 \text{ MHz})$, $(90.035^\circ, 1420 \text{ MHz})$, $(90.04^\circ, 1420 \text{ MHz})$; 1420 MHz pattern results.

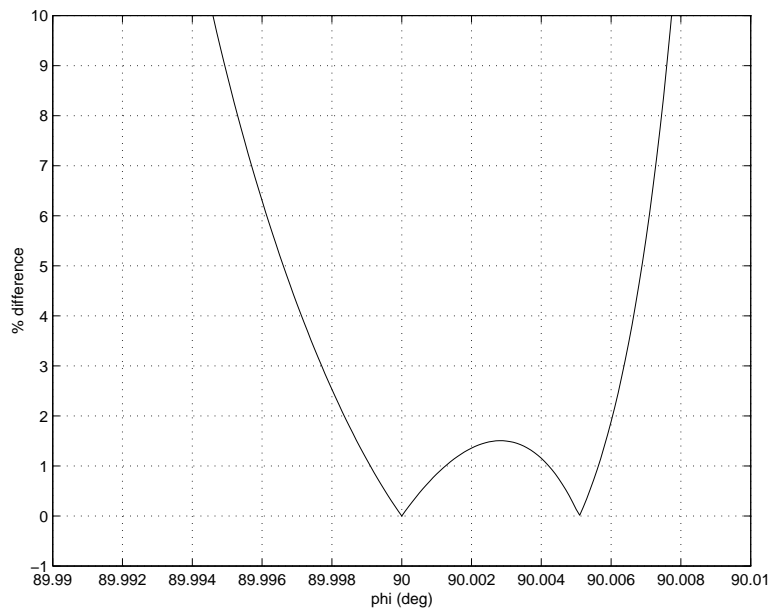
There is a little more pattern distortion in the main lobe, however, the pointing direction constraint is still enforced. Also, as expected, the null broadens dramatically in frequency: It is now on the order of 40 MHz wide.

REFERENCES

- [1] S.W. Ellingson, "Beamforming and Interference Canceling with Very Large Wideband Arrays," *IEEE Trans. Antennas and Propagation*, in press (scheduled to appear in the April 2003 issue; preprint available: <http://esl.eng.ohio-state.edu/people/researchers/ellingson.html>).

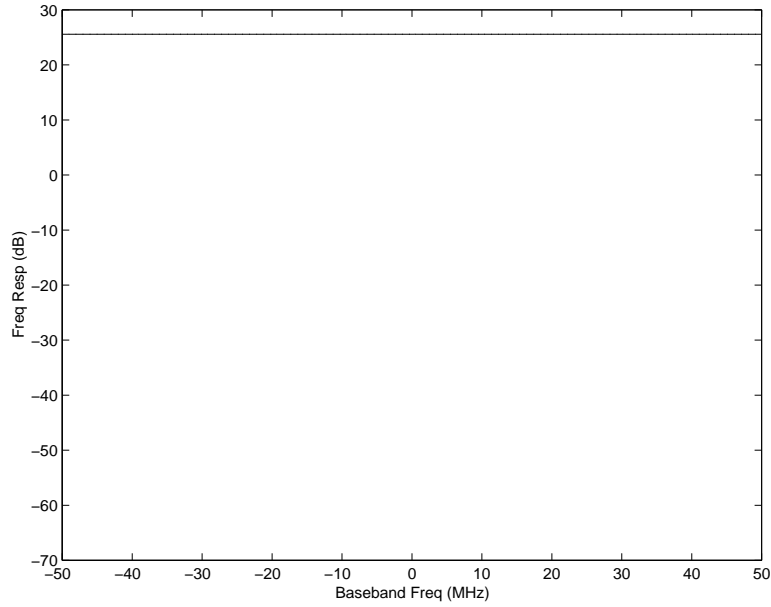


(a) Pattern. *Solid: New, Dash: Prototype.*

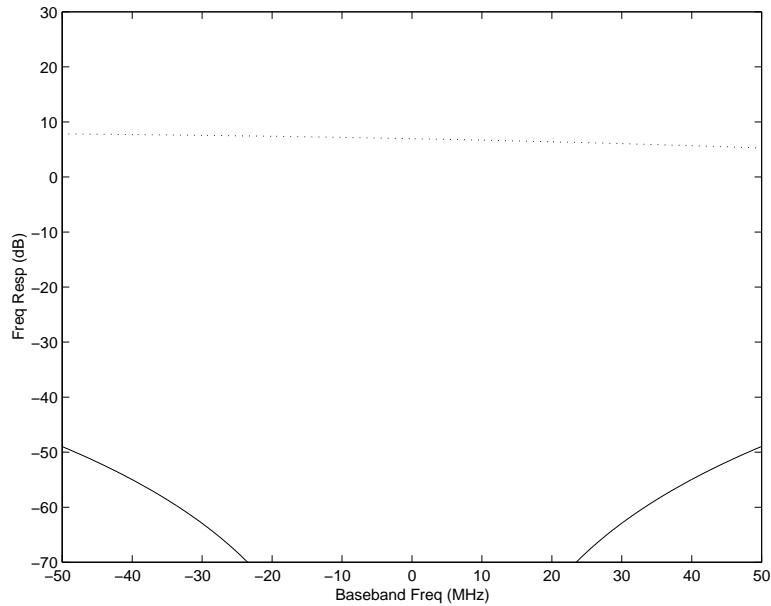


(b) Pattern error in main lobe.

Fig. 4. Three nulls: $(90.03^\circ, 1410 \text{ MHz})$, $(90.03^\circ, 1420 \text{ MHz})$, $(90.03^\circ, 1430 \text{ MHz})$; 1420 MHz pattern results.



(a) Frequency Response at 90.0° . *Solid: New, Dash: Prototype.*



(b) Frequency Response at 90.03° . *Solid: New, Dash: Prototype.*

Fig. 5. Three nulls: ($90.03^\circ, 1410$ MHz), ($90.03^\circ, 1420$ MHz), ($90.03^\circ, 1430$ MHz); Frequency Response.